SLURRY FISCHER-TROPSCH/MOBIL TWO-STAGE PROCESS OF CONVERTING SYNGAS TO HIGH-OCTANE GASOLINE. QUARTERLY REPORT, JULY 1-SEPTEMBER 30, 1981

MOBIL RESEARCH AND DEVELOPMENT CORP.
PAULSBORO, NJ

OCT 1981

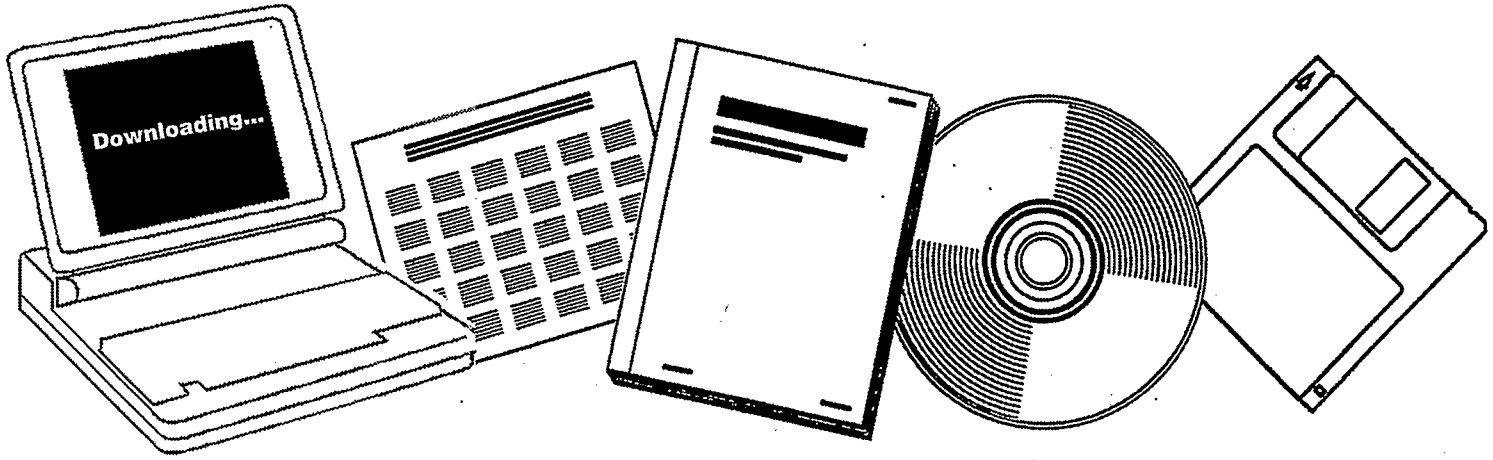

DOE/PC/30022-4
(DE83012404)
Distribution Category UC-90d

SLURRY FISCHER-TROPSCH/MOBIL TWO-STAGE PROCESS OF CONVERTING SYNGAS TO HIGH OCTANE GASOLINE

QUARTERLY REPORT FOR THE PERIOD
1 JULY - 30 SEPTEMBER, 1981

REPORT PREPARED BY: J. C. W. KUO

CONTRIBUTORS:
S. K. ADITYA
K. M. GUPTE
T. M. LEIB

MOBIL RESEARCH AND DEVELOPMENT CORPORATION
PAULSBORO, NEW JERSEY 08066

DATE PUBLISHED - OCTOBER 1981

PREPARED FOR THE UNITED STATES
DEPARTMENT OF ENERGY
UNDER CONTRACT NO. DE-AC22-80PC30022

TABLE OF CONTENTS

I. Abstract

The fabrication of all Bench-Scale Unit (BSU) components in the machine shop is complete. The on-site construction of the BSU has been initiated. The on-site installation of major BSU vessels is complete. And the writing of an operating manual for the BSU has also been initiated.

A mathematical model of the F-T bubble-column reactor containing a description of a liquid-phase axial dispersion has been developed. It is being used to assist the planning and the operation of the BSU. A parametric study was carried out to determine a combination of parameters that gives the largest effect on the F-T reactor performance due to the existence of a liquid-phase axial mixing. In BSU operations, the effect of the liquid-phase axial mixing on the BSU F-T reactor performance is estimated to be small to moderate. A preliminary study shows that the effect of the liquid-phase axial mixing on large-scale reactors can be significant. However, more understanding of the hydrodynamic behavior of large-scale reactors containing internal cooling tubes is needed.

II. Objective and Scope of the Project

The overall objective of the contract is to develop a two-stage slurry Fischer-Tropsch/ZSM-5 process for direct conversion of syngas, of the type produced in a coal gasification system, to high octane gasoline. The immediate objective is to design, construct, and operate a bench-scale pilot plant so that the economic potential of this process concept can be evaluated. To accomplish these objectives, the following specific tasks will be undertaken:

Task 1 - Design of Bench-Scale Pilot Plant

A two-stage slurry F-T/ZSM-5 bench-scale pilot plant will be designed for conversion of syngas to high octane gasoline. The slurry F-T reactor will be 2" ID and and 25' high. The fixed-bed ZSM-5 reactor will be 2" ID and 4-18" high. A distillation column will be designed to obtain stabilized gasoline products.

Task 2 - Construction and Shakedown of Pilot Plant

The pilot plant will be constructed in MRDC Paulsboro Laboratory. The unit will be shaken down when completed.

Task 3 - Operation of Pilot Plant

At least three slurry F-T catalysts will be tested in the bench-scale pilot plant. One of these catalysts may be provided by DOE's alternate catalyst development projects. The best first-stage catalyst together with a ZSM-5 class zeolite catalyst will be used for process variable studies and catalyst aging tests in the bench-scale unit. Products obtained from the unit will be evaluated to define their qualities.

Task 4 - Conceptual Design Study

A preliminary conceptual design of the process will be developed for a commercial size plant for the conversion of syngas to high octane gasoline. Scoping costs of the plant will be estimated.

III. Summary of Progress to Date

The construction phase of the BSU is progressing satisfactorily. The fabrication of major BSU components in the machine shop is complete. The on-site construction of the BSU has been initiated. The major BSU vessels have also been installed on-site. During this period, an additional nineteen BSU construction drawings have been completed.

The writing of an operating manual for the BSU has been initiated and is progressing satisfactorily. The F-T bubble-column mathematical model has been improved to contain a description of the liquid-phase axial mixing. An orthogonal collocation numerical method and an iteration scheme were used to obtain solutions from this model. The following conclusions were drawn after using this model to evaluate the effect of the liquid-phase axial mixing on the F-T bubble-column performance:

- A case of the largest effect due to the liquid-phase axial mixing was identified after a parametric study on all parameters involved in the model.
- Based on the largest effect case, the effect of the liquid-phase axial mixing on the BSU F-T reactor performance is estimated to be small to moderate.
- It is estimated that the effect of the liquid-phase axial mixing on large-scale F-T bubble reactor performance can be significant. However, the hydrodynamic behavior of large-scale reactors containing internal cooling tubes is highly uncertain and further experimentation in this area is recommended.
- The intrinsic kinetic rate constant derived from the conversion data of the Rheinspressen-Koppers F-T demonstration reactor is estimated to be 0.95-1.02 mL Liquid/s-gFe, which is about 2-10% higher than estimations based on non-mixing liquid model.

IV. Detailed Description of Technical Progress

A. Task 2 - Construction and Shakedown of Pilot Plant

1. Status of Task

The F-T slurry-reactor and two fixed-bed reactors have been fabricated; the BSU components fabrication in the machine shop is now complete. The on-site construction of the pilot-plant has been initiated and is proceeding on schedule.

The slurry-reactor has been assembled and mounted on its steel-structure. Two second-stage fixed-bed reactors have also been installed. The rest of the vessels have been mounted on three Unistrut-frames.

As reported previously, the whole unit is divided into four sections:

- Gas Feed (Drawing No. RA-918)
- Slurry F-T Reactor (Drawing No. RA-919)
- Fixed-bed ZSM-5 reactor and product recovery (Drawing No. RA-920)
- Liquid Hydrocarbon Product Distillation

Except for a few minor variations, the vessels and piping associated with sections 1, 3, and 4 have been installed on three separate Unistrut-frames. The slurry-reactor and the associated vessels have been mounted on a separate 43' high steel-structure. For convenience, the two fixed-bed reactors have also been mounted on this structure instead of on the Unistrut-frame corresponding to section 3.

Two elevation-views of the 43' high slurry-reactor steel-structure can be seen in Figure 1. The elevation "A-A" gives the view from the north; while the elevation "B-B" gives the view from the west. The slurry F-T reactor is the tall center piece in two elevation views shown in this figure. The gas-feed pre-heater (E-32) can be seen on the floor next to the slurry-reactor. The slurry-tank (E-48) and slurry transfer vessel (E-49) are placed on the first floor. The inter-reactor sampling-loop components, hot (E-93), and cold (E-94) condensers, sample pots (E-87,88) and gas-meter (E-76) are mounted on the first-floor (see elevation "B-B"). Two fixed-bed reactors (E-36

& 37) are mounted on the outside of the first floor. The three Unistrut-frames for the sections 1,3,4 are located on the north side of the slurry-reactor structure below the fixed-bed reactors (see elevation "A-A").

A view from the north-west side of the pilot-plant under construction can be seen in a photo picture given as Figure 2. The photo shows the steel frame supporting the slurry F-T reactor. A list of pilot plant construction drawings that have been completed during this quarter is given in Table 1.

2. Conclusion

The fabrication of all BSU components including the slurry reactor and two fixed-bed reactors is complete and the on-site contruction is progressing on schedule.

3. Future Work

- The heat-tracing and insulation of the unit will begin after completion of the process piping and pressure testing.
- The electrical wiring and instrumentation for the unit will be completed.

B. Task 3 - Operation of Pilot Plant

1. BSU Pilot Plant Operating Manual

The writing of an operating manual for the BSU has been initiated and is progressing satisfactorily. The manual will be complete by next quarter.

2. Fischer-Tropsch Bubble-Column Mathematical Model and Its Applications

a. An Improvement of the Mathematical Model

The current F-T bubble-column mathematical model has been improved to include a description of axial mixing in the liquid phase. In the last quarterly report (Section IV. B. 1. a.), an approximate axial mixing model, in which a constant superficial gas velocity was set equal to the arithmetic average of the velocities at the column inlet and the column exit, was used. The current model will remove this approximation and give a more accurate description on the axial mixing of the liquid phase.

The model assumptions are the same as those described in the previous quarterly reports. The differential equations representing hydrogen balances in both the gaseous and liquid phases are, respectively, given in dimensionless form as

$$\frac{1+\alpha^*}{(1+\alpha^* \bar{y})^2} \frac{d\bar{y}}{d\bar{z}} + St_d (\bar{y} - \bar{x}) = o \qquad (1)$$

Conversion in Gas Phase — Diffusion from Gas-Liquid Interphase to Liquid

$$Pe_L^{-1} \frac{d^2\bar{x}}{d\bar{z}^2} + K_H St_d (\bar{y} - \bar{x}) - St_k K_H \bar{x} = o \qquad (2)$$

Axial Dispersion in Liquid Phase — Diffusion from Gas-Liquid Interphase to Liquid — Kinetic Dissipation at Catalyst Surface

The boundary conditions are

$$\bar{y} = 1 \quad \text{and} \quad d\bar{x}/d\bar{z} = o \quad \text{at} \quad \bar{z} = o \qquad (3a)$$

$$d\bar{x}/d\bar{z} = o \quad \text{at} \quad \bar{z} = 1 \qquad (3b)$$

The dimensionless variables used above are given in the section of Nomenclature. The coefficient of the first term of Equation (1), $(1+\alpha^*)/(1+\alpha^*\bar{y})^2$, represents the variation of the gas velocity due to the molar contraction resulted from F-T reactions. It is the only cause of non-linearity in the system of Equations (1) to (3). Note that these equations are similar to those described by Deckwer (1980b) except with certain simplifications. Deckwer's model includes three additional features; i.e., axial catalyst distribution, axial temperature gradient, and axial gas-phase dispersion. The effect of the axial catalyst distribution was investigated in the last Quarterly Report and was found to be small for small catalyst particles. The axial temperature gradients in most experiments are small and their effect on the catalyst is small. The effect due to the axial gas-phase dispersion on the bubble-column performance is uncertain and may deserve more detailed evaluation later.

A solution for this set of non-linear equations can be obtained using an orthogonal collocation method (Villadsen and Michelsen, 1978). The use of orthogonal collocation method for solving differential equations is very common in recent years and this method becomes one of the standard numerical methods. Consequently, details of this method are not given here, and are referred to other references, such as Villadsen and Michelsen

(1978) and Finlayson (1980). Basically, the method uses a linear combination of one of the many families of orthogonal polynomials as a trial solution to the dependent variables. In the present application, the Jacobi polynomials with a weighting function $\bar{z}(1-\bar{z})$ are used. This family of polynomials is defined by the following equation:

$$P_j(\bar{z}) = \sum_{i=0}^{j} (-1)^{j-i} \gamma_{ij} \bar{z}^i \tag{4}$$

where

$$\gamma_{0j} = 1 \text{ for all } j \tag{5a}$$

$$\gamma_{ij} = \binom{j-i+1}{i} \binom{j+i+2}{i+1} \gamma_{i-1,j} \tag{5b}$$

The orthogonality relation is given as

$$\int_0^1 \bar{z}\,(1-\bar{z})\,P_i(\bar{z})\,P_j(\bar{z}) = \begin{cases} 0 & \text{if } i \neq j \\ \neq 0 & \text{if } i = j \end{cases} \tag{6}$$

The trial solutions for both $\bar{x}$ and $\bar{y}$, truncated to Nth order polynomials as

$$\bar{x} = \sum_{i=0}^{N+1} a_i P_i(\bar{z}) \tag{7a}$$

$$\bar{y} = \sum_{i=0}^{N+1} a_{N+2+i} P_i(\bar{z}) \tag{7b}$$

are substituted into Equations (1) and (2), and boundary conditions (3a) and (3b). The collocation method dictates that these trial solutions satisfy these equations exactly at the N interior collocation points, which are the zeros of the Nth order polynomial, and at two boundaries. This results in 2(N+2) algebraic equation containing 2(N+2) unknowns. However, the resulting algebraic equations are nonlinear; therefore, an iterative scheme is used to solve these equations. In the current application, the Newton-Raphson routine is used. The criteria of the iteration scheme is that the successive dependent variables at all collocation points and the reactor exit are within 0.1% of each other. Another independent iterative scheme involves a convergence of the hydrogen concentration in the reactor exit, which is used to evaluate some parameters used in the model calculation. The criteria for this iteration is that its successive values are within 1% of each other. It was also found that five collocation points were sufficient to give accurate results in most cases.

b. Effect of Liquid Phase Axial Mixing on BSU F-T Reactor Performance

A preliminary study on the estimated effect of a liquid phase axial mixing on the F-T bubble-column of the BSU was given in the last quarterly report (Section IV. B. 1. a.). An approximate axial dispersion model, in which the superficial gas velocity along the reactor was assumed constant, was used. This approximation results in a set of linear differential equations describing the gas phase and the liquid phase hydrogen concentrations. The solution for those equations can be readily obtained in closed form. However, the results from these calculations were only approximate and may yield inaccurate conclusions. The current, improved mathematical model is used to remove this approximation.

Table 2 lists the parameters adopted in the current mathematical model calculations. To evaluate the effect on the reactor performance due to the axial liquid-phase mixing, a parametric study was done to find out the effect of major parameters on the directional change on the reactor performance. This exercise is essential in establishing a combination of parameters that will give the largest effect on the reactor performance due to the axial liquid-phase mixing. If this case of the largest effect shows a small effect, then it can be concluded that the effect is small in all cases enveloped by the ranges of the parameters under consideration. There are two types of perturbation of these parameters. One type is resulted from the variation within the operational range of parameters, such as the reactor temperature, the reactor pressure, the catalyst loading, the inlet H_2/CO ratio, the superficial feed gas velocity, and the reactor diameter. The other type is the variation of the parameters due to the uncertainty of these parameters, such as the gas bubble size, the gas holdup, the hydrogen solubility, the hydrogen diffusivity, the intrinsic kinetic rate constant, the H_2/CO usage ratio, and the contraction factor. All parameters listed in Table 2 are subjected to parametric study except for the Fe-content in the catalyst, the catalyst solid density, the liquid density and viscosity, the reactor pressure, and the reactor temperature. The first two parameters have very little effect on the calculated effect. The variations of the liquid density and viscosity are reflected in the variation of the liquid-side mass transfer coefficient. Finally, the variation of the reactor temperature is mainly reflected in the variation of the intrinsic kinetic rate constant; while the variation of the reactor pressure is manifested in the variation of the gas velocity.

The base case values of the parameters used in the current study are the same as those used in the last Quarterly Report except for the slightly higher reactor pressure (1.48 mPa

instead of 1.38 mPa). The base case values of the parameters are given in Table 2 together with the ranges of the variations of each parameter. The lower and upper bounds of the gas bubble diameter are those reported by Deckwer, et al. (1980b) and Satterfield and Huff (1980). Those for the liquid-phase hydrogen diffusivity are obtained from the Wilke-Chang correlation (Deckwer, et al., 1980b) and Calderbank, et al. (1963). Those for the hydrogen solubility coefficient and the intrinsic kinetic constant are obtained by varying the base case value by ±50%. Those for the contraction factor are those measured by Deckwer, et al. (1980b). Those for the H_2/CO usage ratio are given arbitrarily but within a reasonable limit. Lastly, the upper bound of the gas holdup is obtained by doubling the base case value.

The liquid-phase axial mixing is described using a constant dispersion coefficient. A correlation of this coefficient recommended by Deckwer, et al. (1980b) is adopted here:

$$E_\ell = 3.676\ u_{gm}^{.32}\ d_R^{1.34} \qquad (8)$$

Note that an arithmetic mean value of the superficial gas velocity is used here. This approximation will result in a maximum deviation on the dispersion coefficient over the whole reactor length of about 10%. The correlation given by Equation (8) contains data obtained with the superficial gas velocity up to 90 cm/s and with the reactor diameter up to 60 cm. Some of this data may very well be in the turbulent flow region. However, most of the data were obtained in systems of air-water, and some were in systems of air-aqueous glycerine. It is not clear if data obtained from these systems can be applied to our present system. In the current study, the calculated effect of the liquid-phase axial mixing described by Equation (8) on the F-T bubble-column performance is compared against those of the Non-Mixing (E_ℓ=0) and the Perfectly-Mixed (E_ℓ=∞) cases.

Table 3 summarizes results of this parametric study. It shows the variations of the parameters that result in an increase of calculated effect on the F-T bubble-column performance due to the existence of the liquid-phase axial mixing. An increase in this effect is measured by an increase of the following parameter

$$(1-X_H^e)_{AD}/(1-X_H^e)_{NM} \qquad (9)$$

where the subscript AD denotes the case with the existence of the liquid-phase axial dispersion and the subscript NM denotes the case of non-mixing liquid-phase. In conclusion, in order to obtain a case that gives the largest effect due to the existence of the liquid-phase axial dispersion, one shall use the

upper-ranged values of the liquid side mass transfer coefficient, the intrinsic kinetic rate constant, the H_2/CO usage ratio, the contraction factor, the liquid-phase hydrogen diffusivity, the catalyst loading in the reactor slurry, the reactor diameter, and the lower-ranged values of the gas bubble size, the gas holdup, the hydrogen solubility coefficient, the feed gas superficial velocity, and the inlet H_2/CO ratio.

The effect of the liquid-phase axial mixing on the BSU F-T reactor performance can now be estimated using the largest effect case at a reactor diameter of 2". The result of this calculation is plotted in Figure 3, given as the hydrogen conversion versus the reactor length. For comparison, the results for both the non-mixing and the perfectly-mixed liquid cases are plotted in the same diagram. The curve representing the largest effect case is, as expected, enveloped on both sides by those of the non-mixing and the perfectly-mixed liquid cases. The perfectly-mixed liquid case deviates substantially from the largest effect case; while the deviation between the non-mixing liquid phase and the largest effect case is small to moderate. In the latter comparison, the reactor length required to achieve a 90% conversion is about 15% longer than that estimated using the non-mixing liquid phase approximation. In conclusion, the liquid-phase axial mixing effect shall be included in the future model calculation.

c. A Preliminary Study of Effect of Liquid-Phase Axial Mixing on Large-Scale F-T Reactor Performance

In a large-scale F-T reactor, the effect of the liquid-phase axial mixing is expected to become larger because of less hindrance from the reactor wall on the liquid movement. However, there are three factors that greatly complicate this issue. The first factor is that, in a large-scale reactor, the operational gas velocity, whose upper bound is determined by the existence of the gas-liquid slug flow in smaller reactors, become substantially higher. With a higher gas velocity, the effect of the liquid-phase becomes less. The second factor is that a large-scale reactor will contain cooling tubes in the reactor to remove the large amount of reaction heat. The existence of the cooling tubes will provide the surfaces that hinder the liquid movement and the effect of the liquid-phase axial mixing. The last factor is the possible existence of the chum-turbulent flow-region in a large-scale high gas velocity reactor (Deckwer, et al., 1980a). More studies, particularly non-reacting flow model experiments, are essential in understanding the hydrodynamic behavior of such systems. In the following, a preliminary study was done using the actual operational data of the 155 cm inside diameter and 8.6 m height Rheinspressen-Koppers demonstration reactor.

To maximize the effect of the calculated liquid-phase axial mixing, the upper bound of the liquid-phase hydrogen diffusivity and the lower bound of the hydrogen solubility coefficient were adopted in the calculation. Assuming that the hydrodynamic description used in the current mathematical model can be applied to this case study, an effective reactor diameter must be estimated to account for the effect due to the existence of the vertical cooling tubes. One may define this effective reactor diameter as the hydraulic diameter of the free flow area, i.e., the equivalent circular diameter that gives the same perimeter-to-flow area ratio. The hydraulic diameter of this reactor is 25.4 cm. However, another effective reactor diameter defined as the equivalent circular diameter that gives the same free flow area has also been proposed. This equivalent diameter is 129 cm, which is substantially different from the hydraulic diameter. It is not clear which definition gives a better representation of the actual phenomenon. However, it is certain that either definitions fail when they are applied to some extreme cases of peculiar configuration of the cooling tubes. The representative effective reactor diameter may lie between these two diameters. In Figure 4, calculated results based on these two diameters are shown together with the two extreme cases of the non-mixing and the perfectly-mixed liquid. Using the hydraulic diameter as the effective reactor diameter results in about 10% longer reactor length than that required in the non-mixing liquid case, while using the free-flow-area diameter results in about 50% longer. This reactor performance is far from the perfectly-mixed liquid-phase case. Note that if the hydraulic diameter is the proper effective reactor diameter for accounting the effect of the vertical cooling tubes, the reactor scale-up problem will become very simple.

In the first quarterly report (October-December, 1980), intrinsic kinetic rate constants for precipitated Fe catalysts were estimated from literature data using both the non-mixing and the perfectly-mixed liquid models. It was stated there that the data from the Rheinspressen-Koppers demonstration plant may have been affected by a significant degree of axial liquid mixing. Table 4 shows the estimated intrinsic rate constants obtained by using these liquid-phase mixing models and the current mathematical model. The estimated kinetic constants from these models are different because the estimated effects due to different liquid-phase mixing are different. In conclusion, the kinetic constant estimated from the model containing the liquid-phase axial mixing results in about 2-10% increase from that of the non-mixing liquid model.

3. Conclusion

The work on writing an operating manual for the BSU has been initiated and is progressing satisfactorily.

An improved F-T bubble-column mathematical model containing a description of the liquid-phase axial mixing has been developed. The resulting differential equations and the associated boundary conditions can be solved using an orthogonal collocation numerical method and a Newton-Raphson iteration scheme. This numerical method gives satisfactory results with five interior collocation points.

This mathematical model was used to evaluate the effect of the liquid-phase axial mixing on the F-T bubble-column performances and the following conclusions were obtained:

- A parametric study was done to identify a case of the largest effect due to the liquid-phase axial mixing. This case occurs by combining the upper bound values of some parameters and the lower bound values of other parameters as given in Table 3.

- The effect of the liquid-phase axial mixing on the BSU F-T reactor performance is estimated to be small to moderate. The mathematical model containing the liquid-phase axial mixing shall be used when accurate results are desired.

- The effect of the liquid-phase axial mixing on large-scale F-T bubble reactor performance can be significant. However, this effect is greatly complicated by the existence of cooling tubes in large-scale reactors. Further experimentation to evaluate the hydrodynamic behavior of large-scale reactors is recommended.

- The intrinsic kinetic rate constant derived from the conversion data of the Rheinspressen-Koppers F-T demonstration reactor is estimated to be 0.95-1.02 mL Liquid/s-gFe, which is about 2-10% higher than the estimation based on a non-mixing liquid model.

4. Future Work

- An operating manual for the BSU operation will be complete.

- Work on a material balance program will be initiated.

- The improvement of the F-T bubble-column mathematical model will be continued to provide better tool to aid in the planning and the operation of the BSU F-T reactor.

V. NOMENCLATURE

a_g	Gas bubble interfacial area, $6\epsilon_g/d_B$, (cm^2 gas-liquid area/mL expanded slurry)
a_i	Coefficients, i=1,2,--, 2(N+2), given in Equation (7)
C_{Fe}	Iron loading, (gFe/mL liquid)
C_H	H_2 concentration, (mol/mL liquid)
$D_{H\ell}$	Liquid-phase H_2 diffusivity, (cm^2/s)
d_B	Bubble diameter, (cm)
d_R	Reactor diameter, (cm)
E_ℓ	Liquid-phase axial dispersion coefficient, (cm^2/s)
f	H_2/CO at reactor inlet
f_{Fe}	Weight fraction of Fe in catalyst
K	$f(1+U)/(1+f)U$
K_H	H_2 solubility coefficient, $C_{Hg}/C_{H\ell}$, (mL liquid/mL gas)
k''_H	Intrinsic kinetic rate constant for H_2 conversion, $r_H/(1-\epsilon_g)(1-v)C_{H\ell}\ C_{Fe}$, (mL liquid/s-gFe)
k_ℓ	Liquid side mass transfer coefficient, (mL liquid/s-(cm^2 gas-liquid area))
L	Bubble column height, (cm)
ℓ	Reactor vertical distance from its entrance, (cm)
N	Number of interior collocation points
P	Pressure, (mPa)
$P_j(\bar{z})$	Jacobi polynomials, j=1,2 --, defined as Equation (4)
R_d	H_2 transport resistance from gas-liquid interface to bulk liquid phase, $K_H/k_\ell a_g$, (s-mL expanded slurry/mL gas)
R_K	Kinetic resistance, $K_H/k''_H C_{Fe}(1-\epsilon_g)(1-v)$, (s-mL expanded slurry/mL gas)

T	Temperature, (°C)
U	H_2/CO usage ratio
u	Superficial velocity, (cm/s)
v	Volumetric fraction of catalysts in slurry, $\rho_\ell w/(\rho_s+w(\rho_\ell-\rho_s))$, (mL catalyst/mL slurry)
w	Weight fraction of catalysts in slurry, (gCat/g slurry)
X_H	H_2 conversion
$\bar{x}$	Dimensionless liquid-phase H_2 concentration, $K_H C_{H\ell}/C_{Hg}^{\ i}$
y	Gas-phase H_2 mole fraction
$\bar{y}$	Dimensionless gas-phase H_2 mole fraction, y/y^i
$\bar{z}$	Dimensionless axial reactor distance, ℓ/L
	Greek Letters
α	Contraction factor, $-\gamma U/(1+U)$
α^*	αK
γ	Moles product per mole of H_2 converted in F-T reaction
γ_{ij}	Coefficients for Jacobi polynomials, i,j = 1,2 --, defined by Equation (5)
ϵ_g	Gas hold-up, (mL gas/mL expanded slurry)
ρ	Density, (g/mL)
ρ_s	Catalyst solid density, (g/mL)
μ	Viscosity, (g/s-cm)
	Dimensionless Numbers
St_d	Stanton number (diffusion resistance), $L/u_g^{\ i}R_d$
St_k	Stanton number (kinetic resistance), $L/u_g^{\ i}R_k$
Pe_L	Peclet number (reactor length), $u_g^{\ i}L/E_\ell(1-\epsilon_g)(1-v)$
	Superscripts
i	At reactor inlet
e	At reactor exit

e	At reactor exit

Subscripts

m	Arithmetic mean value of that at reactor entrance and that at reactor exit.
g	Gas
l	Liquid
c	Catalyst
Fe	Iron

VI. Literature

Calderbank, P. H., Evens, F., Farley, R., Jepson, G., and Poll, A., "Catalysis in Practice", Sym. Proc. (Instr. Chem. Engrs., London), p. 66, (1963).

Deckwer, W. D., Serpeman, Y., Ralek, M., and Schmidt., B., A.I.Ch.E. 73rd Annual Meeting, Chicago (Nov. 1980a).

Deckwer, W. D., Serpeman, Y., Ralek,M., and Schmidt, B., A.I.Ch.E. 73rd Annual Meeting, Chicago (Nov. 1980b).

Finlayson, B. A., "Nonlinear Analysis in Chemical Engineering", McGraw-Hill Inc., New York (1980).

Koelbel, H., and Ralek, M., Cat. Rev. Sci. Eng., 21, 225 (1980).

Satterfield, C., and Huff, G., Chem. Eng. Sci., 35, 195 (1980).

Villadsen, J., and Michelsen, M. L., "Solution of Differential Equations by Polynomial Approximation", Prentice Hall, Inc., Englewood Cliffs, N.J. (1978).

Table 1

LIST OF BSU CONSTRUCTION DRAWINGS COMPLETED DURING THIS QUARTER

Drawing No.	Description
RA-922,923 and 924	Piping and Vessels (P&V) Arrangement for Slurry-Reactor Section 2
RA-929	P&V Arrangement for Section 1
RA-930	Unistrut Structure Frame for Section 1
RA-954	P&V Arrangement for Section 3
RA-955	Unistrut-Structure Frame for Section 3
RA-956	P&V Arrangement for Section 4
RA-957	Unistrut-Structure Frame for Section 4
RB-9100	Glycol-System Piping Diagram
RB-9296	Air-Supply Consoles
RB-9096	Instrument Console
RC-4537	Unit Lighting Arrangement
RB-9300 through 9304 & RD-2772	Electrical Diagrams

Table 2

PARAMETERS AND THEIR RANGES ADOPTED IN THE CURRENT F-T REACTOR MATHEMATICAL MODEL CALCULATIONS

Parameters	Base Case	Ranges
Hydrodynamic Parameters		
d_B, (cm)	.07	.07-.25
k_ℓ, (cm/s)	.02	.02-.09
ϵ_g	$.053(u_{gm})^{1.1}$	$(.053-.106)(u_{gm})^{1.1}$
Reaction Parameters		
k_H'', (mL Liquid/s-gFe)	1.1	.5-2.0
U	.645	.6-.69
$-\alpha$	.5	.5-.6
Physical Parameters		
$D_{H\ell}$, (cm^2/s)	10^{-4}	10^{-4}-10^{-3}
f_{Fe}	.67	-
K_H (mL Liquid/mL Gas)	4.4	2.2-6.6
ρ_ℓ, (g/mL)	.667	-
ρ_s (g/mL)	5.2	-
μ_ℓ, (g/s-cm)	.022	-
Operation Parameters		
d_R, (cm)	5.08	5.08-1.29
f	.7	.6-.7
P, (mPa)	1.48	-
T, (^oC)	265	-
u_g^i, (cm/s)	4	2-9.5
wt_{Fe}	.10	.05-.20

Table 3

VARIATION OF PARAMETERS THAT RESULTS IN AN INCREASE ON THE CALCULATED EFFECT OF THE LIQUID-PHASE AXIAL MIXING ON THE F-T BUBBLE-COLUMN PERFORMANCE

Parameters	Variation(1)
Hydrodynamic Parameters	
d_B	D
E_ℓ	I
k_ℓ	I
ϵ_g	D
Reaction Parameters	
k_H''	I
U	I
$-\alpha$	D
Dimensionless Parameters	
Pe_L	D
St_d	I
St_k	I
Physical Parameters	
$D_{H\ell}$	I
K_H	D
Operation Parameters	
d_R	I
f	D
$u_g{}^i$	D
wt_{FE}	I
$L(1-\epsilon_g)$	I

(1) "D" denotes a decreasing and "I" denotes an increasing value of the parameter defined by (9).

Table 4

ESTIMATED KINETIC RATE CONSTANTS DERIVED FROM DATA OF RHEINSPRESSEN-KOPPERS DEMONSTRATION PLANT USING DIFFERENT LIQUID-PHASE MIXING MODELS[1]

	Liquid-Phase Axial Mixing Models		
Intrinsic Kinetic Rate Constant	Non-Mixing	With Axial Mixing	Perfectly-Mixed
k_H''	.93	.95[2]	2.09

[1] Data from Koelbel and Ralek (1980).

[2] This value is based on using the equivalent hydraulic diameter (25.4 cm) as the effective reactor diameter. Using the free-flow area diameter as the effective reactor diameter gives a value of 1.02.

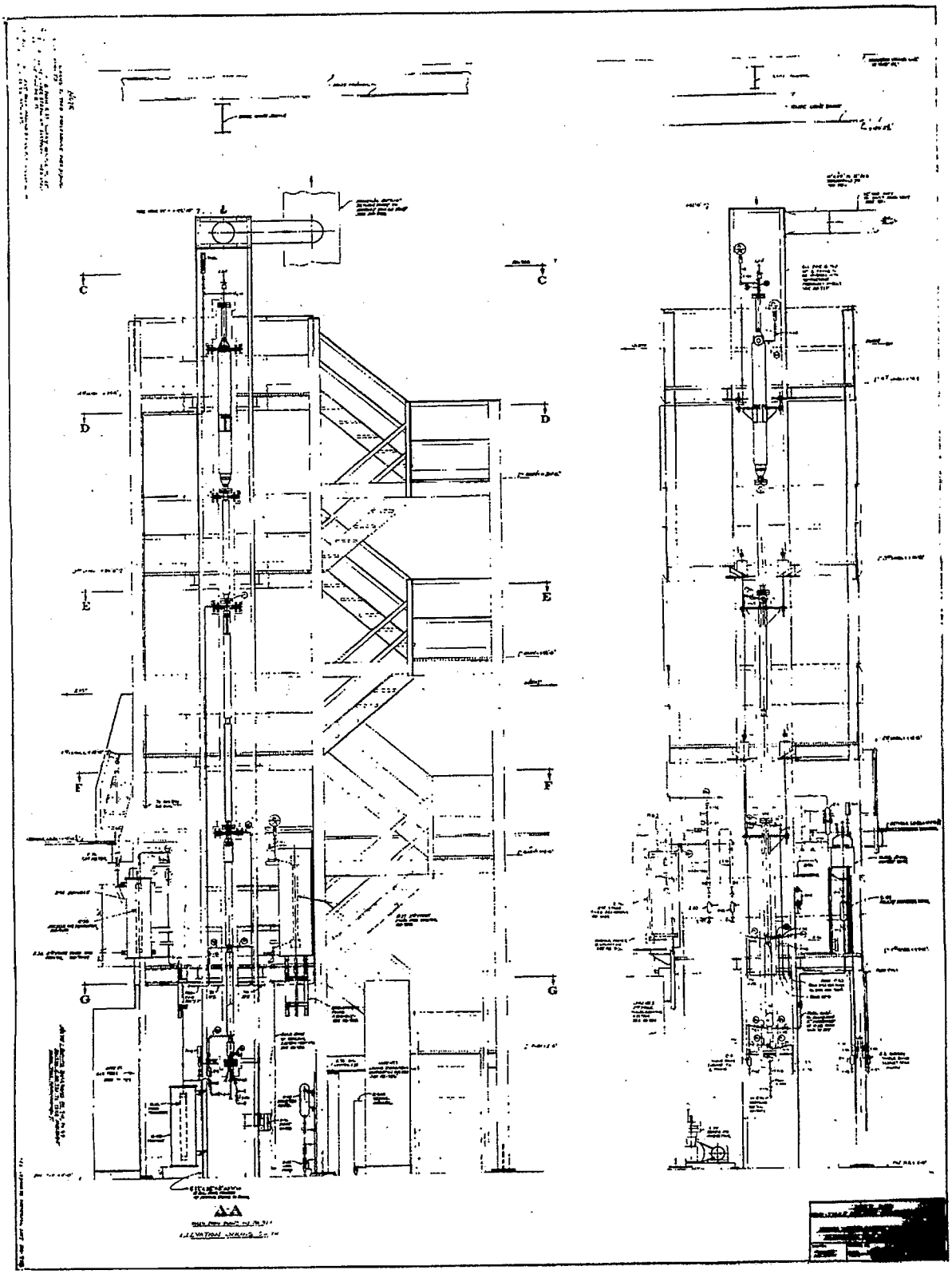

Figure 1 - Elevation Views of the Bench-Scale Pilot Plant

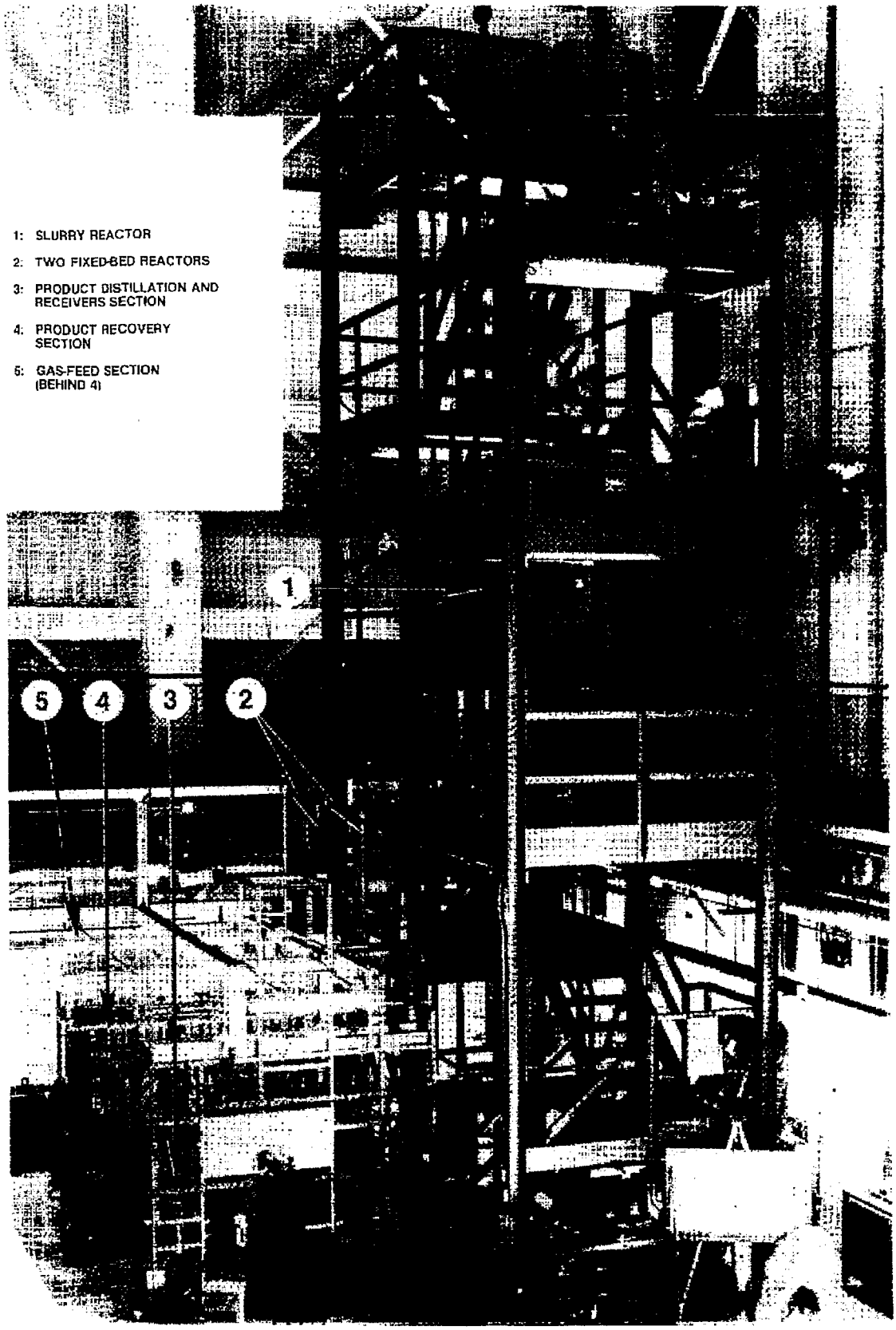

Figure 2 TWO-STAGE FISCHER—TROPSCH AND ZSM-5 SYNGAS CONVERSION BENCH-SCALE UNIT

Figure 3

EFFECT OF AXIAL LIQUID MIXING ON BSU F-T REACTOR PERFORMANCE

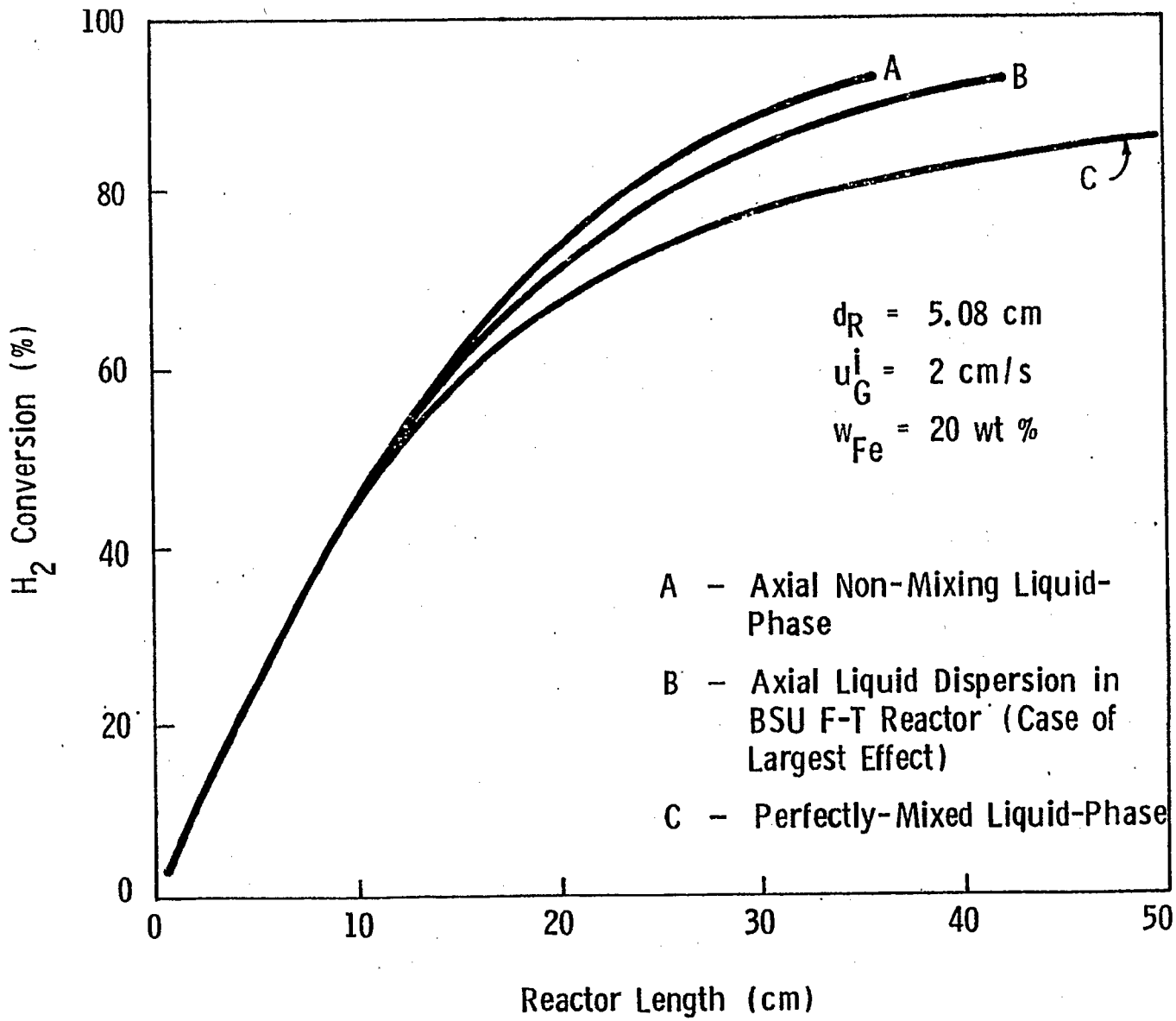

Figure 4

EFFECT OF AXIAL LIQUID MIXING ON LARGE-SCALE F-T REACTOR PERFORMANCE

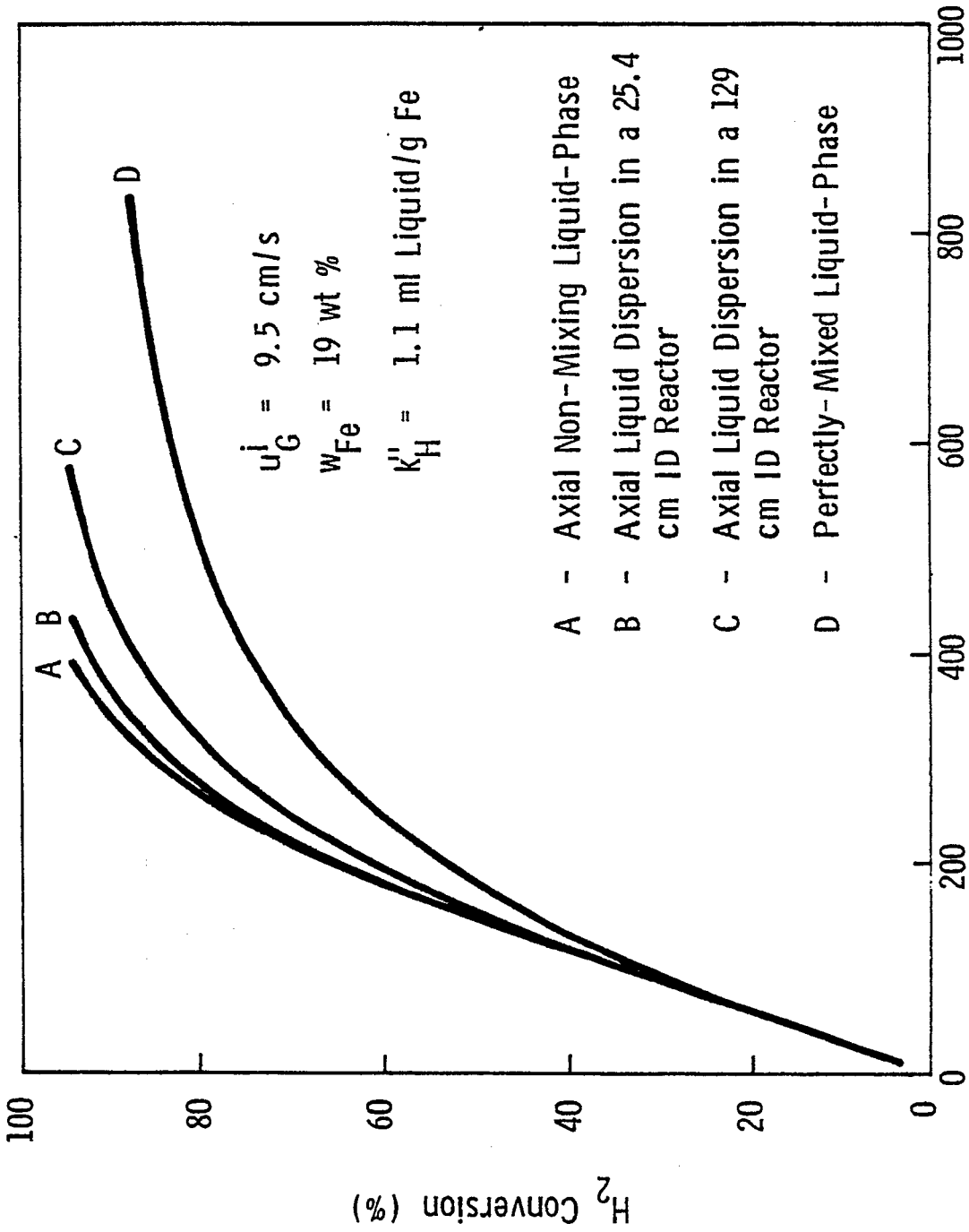

☆U.S. GOVERNMENT PRINTING OFFICE 1983 646 069 863